3. Results

3.1 Micro structure of the conduit

SEM images (Fig. 3) revealed that the wall of the conduit was constructed by overlapped thin mesh layers; every single layer was constituted by randomly crossed chitosan fibers sized from dozens of nanometers to almost 2 micrometers, Interspace between the fibers connected with each other and distributed throughout the structure resulting in a fibrous porous architecture similar to extra cellular matrix (ECM). The laser-drilled pores perforated the whole mesh layers with smooth fused edges. Average pore size was calculated at 200±12 μm and the distance between the centers of 2 neighbored pores was 1±0.04 mm.

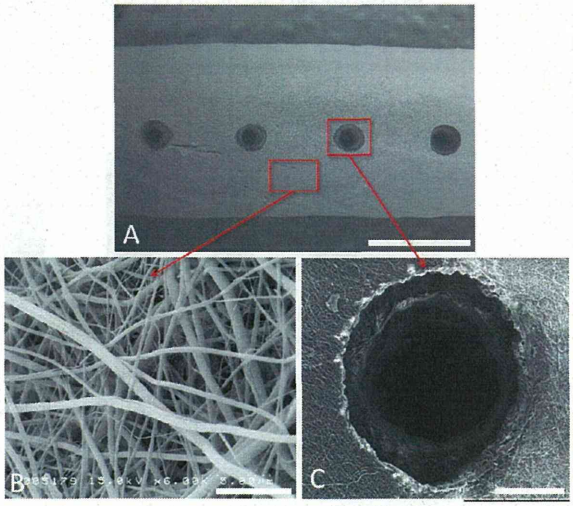

Fig. 3: SEM views of laser drilled nonwoven chitosan conduit. The conduit wall was constructed by many randomly crossed chitosan fibers sized from dozens of nanometers to almost 2 micrometers (B). (C) showed an amplified perforating pore, smooth fused edges of several nonwoven mesh layers could be seen. Average pore size was calculated at 200±12 μm. Scale bars in A, B and C is 1mm, 5 μm and 100 μm respectively.

3.2 Functional recovery

Von Frey hair test in rats records the reaction to a certain tactile stimulation, its value relates to both sensory and motor nerve function of the lower limb (19). It is easy performable and highly reliable compared to other functional tests. The result of Von Frey hair test was shown in (Fig. 4); functional loss after 12 weeks remained in approximately 15% in all experimental groups, Isographs showed a slight improvement yet statistical difference was not detected.

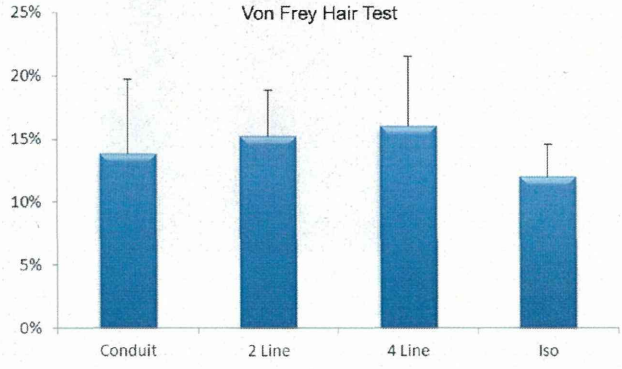

Fig. 4: Results of Von Frey hair test. Functional loss after 12 weeks remained in approximately 15% in

all experimental groups, Isographs showed a slightly better result yet statistical difference was not detected.

3.3 Electrical conductivity of regenerated nerve

CAPs latency is related to nerve conduction velocity, it is considered as a parameter of maturation; when myelinated axons increase it shortens. And amplitude reflects the total number of regenerated axons, when the number of regenerated axons grows it increases (21-22). A similar pattern was obtained with the 2 parameters in our results; conductive function loss remained about 35% after 12 weeks in conduits implanted groups without much difference between each other, Isografts receives the best results at approximately 23%, but no statistical significance was found (Fig. 5).

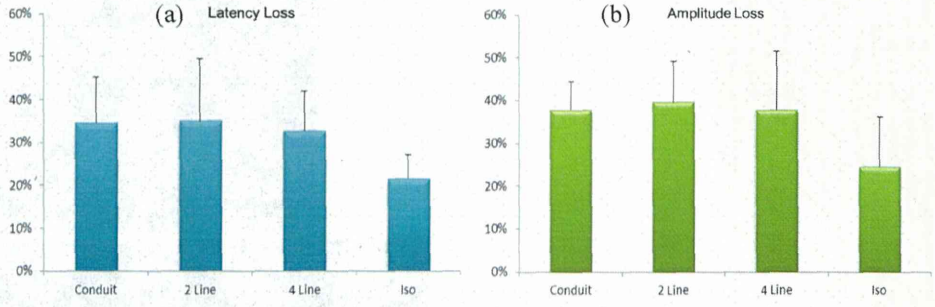

Fig. 5: Results of electro conductivity measurements. A similar pattern was obtained with either the latency (a) or the amplitude (b): conductive function loss remained about 35% after 12 weeks in conduits implanted groups without much difference between each other, Isografts receives the best results at approximately 23%, but no statistical significance was found.

3.4 Histomorphometric analysis of regenerated axon and vessel

Samples harvested at 4 weeks after implantation showed that many small vessels were passing through the pierced pores in a radial pattern (Fig. 6a). Sections cut longitudinally at the pores showed blood vessels penetrated through the pores from outside with some accompanied granulation tissue (Fig. 6b, 6c).

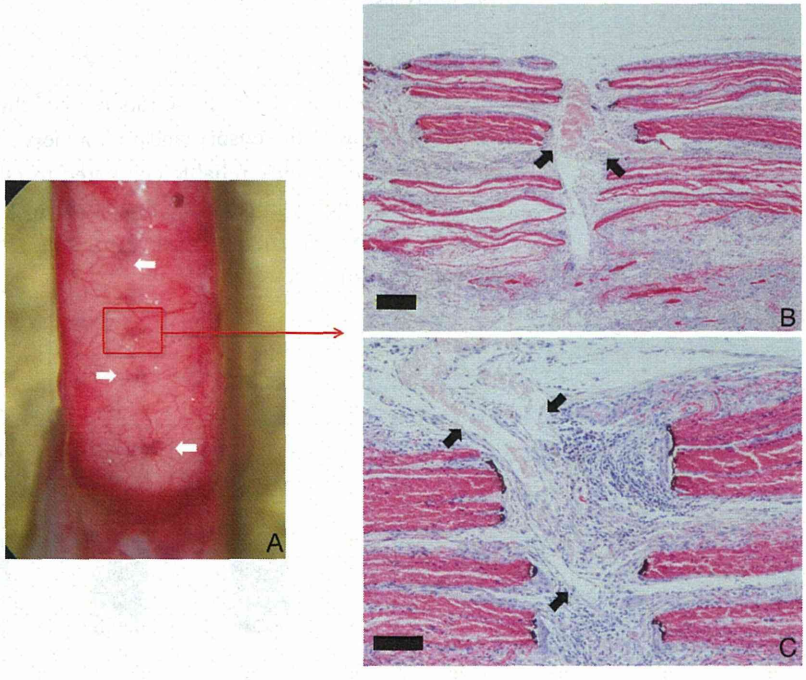

Fig. 6: Gross (A) and histological view (B, C) of the pore-drilled sample harvested at 4 weeks after

implantation. Many small vessels (white arrows in A) were entering the perforating pores in a radial pattern, blood vessels (black arrows in B, C) from outside passed through the pores with some accompanied granulation tissue. HE stain, scale bars in B, C is 200 μm and 100 μm.

Thin Epon sections of samples harvested at 12 weeks post operation revealed that all experimental groups presented vigorous axon regeneration; in the non-pore conduit group, a large number of myelinated axons with various sizes distributed in the lumen with a condensed center (Fig. 7a). Meanwhile, in pore-drilled groups (either in 2 lines or in 4 lines) regenerated axons tended to form fasciculi with endoneurium-like connective tissue sheaths surrounded. Filling of connective fibrous tissue was found very mild and displayed no difference with non-pore group (Fig. 7b, 7c). However, the isograft group presented the most intensive axon regeneration that occupied all the graft cross-sectional area (Fig. 7d).

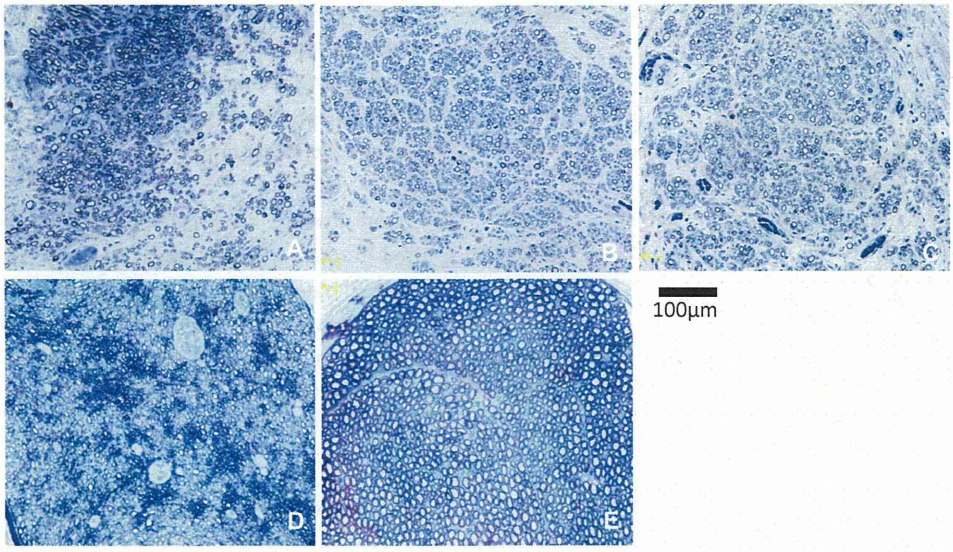

Fig. 7: Transactional view of the midpoint of samples harvested at 12 weeks after implantation. Samples are arrayed from A-E in following group order: non-pore, 2-line pores, 4-line pores, isograft and normal nerve. All experimental groups presented vigorous axon regeneration, in the non-pore conduit group (A), a large number of myelinated axons with various sizes distributed in the lumen with a condensed center; in pore-drilled groups (B, C) regenerated axons tended to form fasciculi with endoneurium-like connective tissue sheaths surrounded; the isograft group (D) presented the most intensive axon regeneration that occupied all the graft cross-sectional area. Epon thin section stained with toluidine blue.

Vessel counting indicated that the average diameter of neovascularized vessels inside the grafts varied from 7 to 13 μm, pore-drilled conduits had a tendency to present larger vessels than the other groups, yet there was no statistical significance (Fig. 8a). However, the results of vessel density measurement showed a gradient increase of vessel density in the order of non-pore conduit, conduit with 2 lines of pores, conduit with 4 lines of pores, Isograft and normal nerve. There were significant differences between the nerve conduits and Isograft or normal nerve, but with more pores opened the significance decreased, there was no significant difference between conduit with 4 lines of pores and Isograft (Fig. 8b). The effect of introducing blood vessels into lumen regenerating space by drilling perforating pores was confirmed.

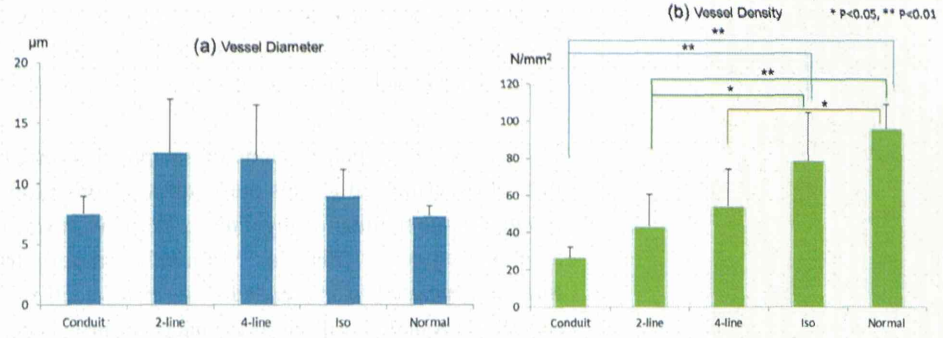

Fig. 8: Results of vessel measurements after 12 weeks of implantation. Vessel diameter was shown in (8a), they varied from 7 to 13 μm, conduits with pores had a tendency to present larger vessels than the other groups, yet there was no statistical significance. Vessel density was shown in (8b), a gradient increase of vessel density was presented in the order of non-pore conduit, conduit with 2 lines of pores, conduit with 4 lines of pores, Isograft and normal nerve. There were significant differences between the nerve conduits and Isograft or normal nerve, but with more pores opened the significance decreased, there was no significant difference between conduit with 4 lines of pores and Isograft.

The axon analysis suggested that there were no significant differences of axon size in all grafted groups; Average axon diameters from grafted groups were at 1.6 to 1.7 μm, reached approximately half the size of normal nerve (3.1 μm) at 12 weeks post operation (Fig. 9a). Meanwhile with regard to axon density, Isograft showed an outstanding abundance with the number of $5.1*10^4/mm^2$, leave the other groups far behind with their value at about $2.7*10^4/mm^2$. No differences were showed in the rest groups; however the slightly low number of normal nerve in density was considered rising from its large axon size (Fig. 9b).

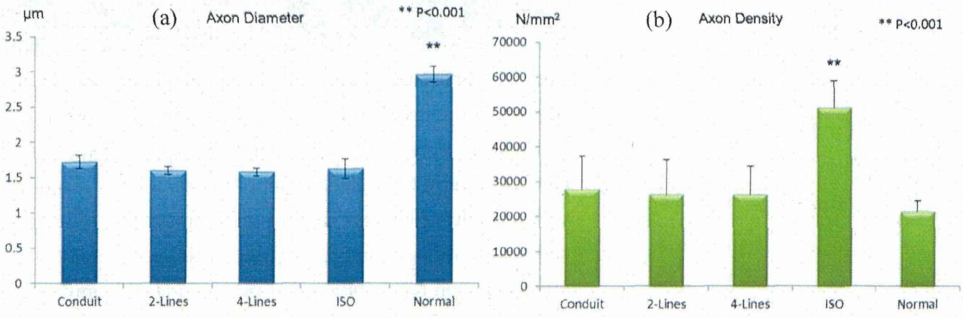

Fig. 9: Results of axon assessments at 12 weeks after implantation. Axon size was shown in (9a), there were no significant differences of axon size in all grafted groups, and they reached approximately half the size of normal nerve ($P<0.001$). Axon density was shown in (9b), isograft showed an outstanding abundance, leave the other groups far behind ($P<0.001$). No differences were found in the rest groups.

4. Discussions

In recent years, electrospinning has been extensively used to construct tissue-engineered scaffolds; it is a simple fabrication process that can easily produce nanofibrous scaffolds which are a suitable environment for cell attachment and proliferation due to their mimetic topographical features to extra cellular matrix (ECM) (23). Many reports including our previous research have demonstrated the advantages of inducing nanofiber orientation on peripheral nerve regeneration (10, 24-26), the nerve conduits fabricated by nonwoven mesh of aligned nanofibers showed better guidance of neurite ingrowth resulting in matched nerve regeneration with isograft. The reason we didn't apply

oriented nanofibrous chitosan mesh conduit in this study is from the concern that it is more convenient for a negative control to receive moderate results, to display the power of the factors that we are really interested in, which in this study is the function of perforating pores.

The regrowth of new blood vessels into tissue defects, in term of neovascularization, plays a crucial role in tissue regeneration and repair. One of the major reasons that regenerative tissue in large volume still remained a big challenge is the difficulty of guaranteeing rapid and sufficient neovascularization to support the whole regenerating process simultaneously. Several approaches to enhance revascularization were proposed like seeding of endothelia, administrating of vascular growth factors (VEGF, FGF), and stimulating slight inflammatory reaction accompanied with angiogenesis by biochemical reagents (27-30), none of them is easily accomplishable. Compared to dense biomaterials, porous bioscaffolds with interconnected inner pores provide better tissue ingrowth and integration as well as faster degeneration (31-34). Because body tissues have the tendency to fill up defect cavities with granulation tissue accompanied by neovascularization, it is reasonable to consider that through introducing perforating pores to a chamber structure inside body, the lumen contents could receive more vascular supply from surrounding tissues, and when the pore size is controlled properly the infiltration of fibrous tissue could be inhibited at a low level.

There are many literatures concerning the influences of pore sizes with different porous biomaterials (35-37). Pore sizes at 200-300 μm were considered favoring neovascularization (38-39), pore sizes of <200 μm were found to be watertight hindering liquid circulation (40) and pores of <100 μm only lead to ingrowth of single cell types instead of building up new tissues (41-43). For the accurate process of pore opening, we applied laser drilling technology which has the advantages of precision, cleanness and efficiency. We determined the pore size at 200 μm for 2 reasons: it is reported favoring neovascularization but not large enough to induce mass unfavorable fibrous tissue; after several tests of the Laser Marker, we found the minimal energy and duration setting to ensure an even penetrating pore through the whole chitosan mesh wall gave the pore size at about 200 μm. No more than 4 lines of pores (40 pores/conduit) were drilled is because of the worries of reducing conduit mechanical intensity and promoting infiltration of fibrous connective tissue.

Our grafting results suggested that by introducing perforating pores, blood supply from surrounding environment was enhanced with small vessel ingrowth and the effect depended on pore density. For peripheral nerve conduit, wall pore size at 200 μm with the density of 40/cm didn't cause obvious fibrous tissue invasion that hindering nerve regeneration. Accompanying the improved vascularization, enhancement of axon regeneration was not shown with the parameters of axon diameter and density, but morphological changes of presenting more matured fasciculi were observed.

The reasons may lie in good function of the control group, nonwoven chitosan mesh conduit, which has permeability itself and a high compatibility to neurite elongation; and also in a relatively short graft distance that could not reveal the differences. Permeation of the mesh architecture and the blood supply from the proximal/distal stumps may support the regeneration enough in a short mesh graft at the length of 12mm. Thus a longer defect model with other nerve guidance conduit is considered to be employed in further studies.

The organization of fascicular structures of axon bunds could indicate the level of maturity and functional complexity (44, 45). Different fascicles supply specific muscles and cutaneous areas, fascicularization and topography has substantial clinical relevance in nerve functions (46-49). In this study our open porous conduits not only promoted vessel ingrowth but also provided the accompanying connective tissue which facilitates the formation of fascicular sheaths, resulting in more matured histological view with the feature

of noticeable minifascicle formation. So the pore opened conduits were considered to exhibit a more natural fashion of compound tissue regeneration.

Isograft's ascendancy comes not only from the abundance of revascularization but also from the numerous guidance channels of residual basement membrane which contains many neural adhesion molecules like Laminin and Integrin. This is partially proved in our previous study with laminin coated chitosan nonvowen conduit which received comparable results with Isograft (50).

5. Conclusion

By inducing perforating pores to chitosan nonwoven conduit with laser process, conduit revascularization was improved without obvious fibrous tissue infiltration by vessel ingrowth from surrounding tissue through the pores. However except for the maturation of fasciculi, contemporary major nerve regenerative improvements were not observed. Perforating pores may help long conduits without permeability more instead of short permeable conduits.

Acknowledgements

The nonwoven chitosan mesh conduits were kindly provided by Hokkaido Soda Co., Ltd., Hokkaido, Japan. And the laser-drilling processing is supported by Keyence Corp., Tokyo, Japan.

References

1. Kemp SW, Syed S, Walsh W, Zochodne DW, Midha R. Collagen nerve conduits promote enhanced axonal regeneration, schwann cell association, and neovascularization compared to silicone conduits. Tissue Eng Part A. 2009 Aug; 15(8):1975-88.

2. Hashimoto T, Suzuki Y, Kitada M, Kataoka K, Wu S, Suzuki K, Endo K, Nishimura Y, Ide C. Peripheral nerve regeneration through alginate gel: Analysis of early outgrowth and late increase in diameter of regenerating axons. Exp Brain Res 2002; 146:356–368.

3. Suzuki Y, Tanihara M, Ohnishi K, Suzuki K, Endo K, Nishimura Y. Cat peripheral nerve regeneration across 50 mm gap repaired with a novel nerve guide composed of freeze-dried alginate gel. Neurosci Lett 1999; 259:5–78.

4. Itoh S, Suzuki M, Yamaguchi I, Takakuda K, Kobayashi H, Shinomiya K, Tanaka J. Development of a nerve scaffold using a tendon chitosan tube. Artif Organs 2003; 27: 1079-1088.

5. Mackinnon SE, Dellon AL. Clinical nerve reconstruction with a bioabsorbable polyglycolic acid tube. Plast Reconstr Surg 1990;85:419–24.

6. Toba T, Nakamura T, Shimizu Y, Matsumoto K, Ohnishi K, Fukuda S, Yoshitani M, Ueda H, Hori Y, Endo K. Regeneration of canine peroneal nerve with the use of a polyglycolic acid-collagen tube filled with laminin-soaked collagen sponge: A comparative study of collagen sponge and collagen fibers as filling materials for nerve conduits. J Biomed Mater Res 2001; 58:622–630.

7. Giraudguille MM. Fine-structure of the chitin protein system in the crab cuticle. Tissue Cell 1984;16:75–92

8. Yamaguchi I, Itoh S, Suzuki M, Sakane M, Osaka A, Tanaka J. The chitosan prepared from crab tendon I: the characterization and the mechanical properties. Biomaterials 2003;24: 2031–2036.

9. Prabhakaran MP, Venugopal JR, Chyan TT, Hai LB, Chan CK, Lim AY, Ramakrishna S. Electrospun biocomposite nanofibrous scaffolds for neural tissue engineering. Tissue Eng Part A. 2008 Nov;14(11):1787-97.

10. Wang W, Itoh S, Matsuda A, Ichinose S, Shinomiya K, Hata Y, Tanaka J. Influences of mechanical properties and permeability on chitosan nano/microfiber mesh tubes as a

scaffold for nerve regeneration. J Biomed Mater Res A 2008 Feb; 84(2):557-66
11.Wang W, Itoh S, Yamamoto N, Okawa A, Nagai A, Yamashita K Enhancement of nerve regeneration along a chitosan nanofiber mesh tube on which electrically polarized beta-tricalcium phosphate particles are immobilized. Acta Biomater. 2010 Oct;6(10):4027-33. Epub 2010 May 6.
12. Soker S, Machado M, Atala A. Systems for therapeutic angiogenesis in tissue engineering. World J Urol. 2000 Feb; 18(1):10-8.
13. Djonov V, Baum O, Burri PH. Vascular remodeling by intussusceptive angiogenesis. Cell Tissue. Res 2003; 314:107–117. [PubMed: 14574551]
14. Kaully T, Kaufman-Francis K, Lesman A, Levenberg S. Vascularization-the conduit to viable engineered tissues. Tissue Eng Part B Rev. 2009 Jun;15(2):159-6
15. Carruth JA. Lasers in medicine and surgery. J Med Eng Technol. 1984 Jul-Aug;8(4):161-7.
16. Ovsianikov A, Malinauskas M, Schlie S, Chichkov B, Gittard S, Narayan R, Löbler M, Sternberg K, Schmitz KP, Haverich. A Three-dimensional laser micro- and nano-structuring of acrylated poly(ethylene glycol) materials and evaluation of their cytoxicity for tissue engineering applications. Acta Biomater. 2011 Mar; 7(3):967-74. Epub 2010 Oct 25.
17. Xie J, MacEwan MR, Schwartz AG, Xia Y. Electrospun nanofibers for neural tissue engineering. Nanoscale. 2010 Jan 8;2(1):35-44.
18. Wang CY, Zhang KH, Fan CY, Mo XM, Ruan HJ, Li FF. Aligned natural-synthetic polyblend nanofibers for peripheral nerve regeneration. Acta Biomater. 2011 Feb; 7(2):634-43.
19. Bove G.Mechanical sensory threshold testing using nylon monofilaments: the pain field's "tin standard". Pain. 2006 Sep;124(1-2):13-7.
20. Kim YT, Haftel VK, Kumar S, Bellamkonda RV. The role of aligned polymer fiber-based constructs in the bridging of long peripheral nerve gaps. Biomaterials. 2008 Jul; 29(21):3117-27. Epub 2008 Apr 29
21. English AW, Chen Y, Carp JS, Wolpaw JR, Chen XY. Recovery of electromyographic activity after transection and surgical repair of the rat sciatic nerve. J Neurophysiol. 2007 Feb;97(2):1127-34. Epub 2006 Nov 22.
22. Krarup C. Compound sensory action potential in normal and pathological human nerves. Muscle Nerve. 2004 Apr;29(4):465-83.
23. Ceuna S, Tos P, Battiston B. International review of Neurobiology: Essays on Peripheral Nerve Repair and Regeneration (vol. 87). In: Chiono V, Tonda-Turo C, Ciardelli G. Artificial Scaffolds for Peripheral Nerve Regeneration p. 185-186.
24. Smith IO, Liu XH, Smith LA, Ma PX. Nanostructured polymer scaffolds for tissue engineering and regenerative medicine. Wiley Interdiscip Rev Nanomed Nanobiotechnol. 2009 Mar-Apr;1(2):226-36.
25. Biazar E, Khorasani MT, Montazeri N, Pourshamsian K, Daliri M, Rezaei M, Jabarvand M, Khoshzaban A, Heidari S, Jafarpour M, Roviemiab Z. Types of neural guides and using nanotechnology for peripheral nerve reconstruction. Int J Nanomedicine. 2010 Oct 21;5:839-52.
26. Wang W, Itoh S, Konno K, Kikkawa T, Ichinose S, Sakai K, Ohkuma T, Watabe K. Effects of Schwann cell alignment along the oriented electrospun chitosan nanofibers on nerve regeneration. J Biomed Mater Res A. 2009 Dec 15;91(4):994-1005.
27. Glotzbach JP, Levi B, Wong VW, Longaker MT, Gurtner GC The basic science of vascular biology: implications for the practicing surgeon. Plast Reconstr Surg. 2010 Nov;126(5):1528-38.
28. Nomi M, Atala A, Coppi PD, Soker S. Principals of neovascularization for tissue engineering. .Mol Aspects Med. 2002 Dec;23(6):463-83.
29. Hegen A, Blois A, Tiron CE, Hellesøy M, Micklem DR, Nör JE, Akslen LA, Lorens JB.

Efficient in vivo vascularization of tissue-engineering scaffolds. J Tissue Eng Regen Med. 2010 Sep 23.

30. Druecke D, Langer S, Lamme E, Pieper J, Ugarkovic M, Steinau HU, Homann HH. Neovascularization of poly(ether ester) block-copolymer scaffolds in vivo: long-term investigations using intravital fluorescent microscopy. J Biomed Mater Res A. 2004 Jan 1;68(1):10-8.

31. Ifkovits JL, Sundararaghavan HG, Burdick JA .Electrospinning fibrous polymer scaffolds for tissue engineering and cell culture. J Vis Exp. 2009 Oct 21;(32). pii: 1589.

32. Zhu X, Cui W, Li X, Jin Y. Electrospun fibrous mats with high porosity as potential scaffolds for skin tissue engineering. Biomacromolecules. 2008 Jul;9(7):1795-801.

33. Ju YM, Park K, Son JS, Kim JJ, Rhie JW, Han DK Beneficial effect of hydrophilized porous polymer scaffolds in tissue-engineered cartilage formation. J Biomed Mater Res B Appl Biomater. 2008 Apr;85(1):252-60.

34. Laschke MW, Strohe A, Scheuer C, Eglin D, Verrier S, Alini M, Pohlemann T, Menger MD. In vivo biocompatibility and vascularization of biodegradable porous polyurethane scaffolds for tissue engineering. Acta Biomater. 2009 Jul;5(6):1991-2001.

35. Lowery JL, Datta N, Rutledge GC. Effect of fiber diameter, pore size and seeding method on growth of human dermal fibroblasts in electrospun poly(epsilon-caprolactone) fibrous mats. Biomaterials. 2010 Jan;31(3):491-504.

36. Karageorgiou V, Kaplan D. Porosity of 3D biomaterial scaffolds and osteogenesis. Biomaterials. 2005 Sep;26(27):5474-91.

37. Mühl T, Binnebösel M, Klinge U, Goedderz T. New objective measurement to characterize the porosity of textile implants. J Biomed Mater Res B Appl Biomater. 2008 Jan;84(1):176-83.

38. Feng B, Jinkang Z, Zhen W, Jianxi L, Jiang C, Jian L, Guolin M, Xin D The effect of pore size on tissue ingrowth and neovascularization in porous bioceramics of controlled architecture in vivo. Biomed Mater. 2011 Feb;6(1):015007.

39. Cooper JA, Lu HH, Ko FK, Freeman JW, Laurencin CT Fiber-based tissue-engineered scaffold for ligament replacement: design considerations and in vitro evaluation. Biomaterials. 2005 May;26(13):1523-32.

40. Deng X, Guidoin R. Alternative blood conduits: assessment of whether the porosity of synthetic prostheses is the key to long-term biofunctionality. Med Biol Eng Comput. 2000 Mar;38(2):219-25.

41. Bragdon CR,Burke D,Lowenstein JD,O'Connor DO,Ramamurti B,Jasty M,Harris WH. Differences in stiffness of the interface between a cementless porous implant and cancellous bone in vivo in dogs due to varying amounts of implant motion. J Arthroplasty 1996;11(8): 945–951.

42. Zellin G, Linde A. Effects of different osteopromotive membrane porosities on experimental bone neogenesis in rats. Biomaterials 1996;17(7): 695–702.

43. Bertheville B. Porous single-phase NiTi processed under Ca reducing vapor for use as a bone graft substitute. Biomaterials 2006; 27(8): 1246–1250.

44. Stewart JD. Peripheral nerve fascicles: anatomy and clinical relevance. Muscle Nerve. 2003 Nov; 28(5):525-41.

45. Badia J, Pascual-Font A, Vivó M, Udina E, Navarro X. Topographical distribution of motor fascicles in the sciatic-tibial nerve of the rat. Muscle Nerve. 2010 Aug; 42(2):192-201.

46. Hallin RG. Microneurography in relation to intraneural topography: somatotopic organisation of median nerve fascicles in humans. J Neurol Neurosurg Psychiatry. 1990 Sep; 53(9):736-44.

47. Hallin RG, Wu G. Fitting pieces in the peripheral nerve puzzle. Exp Neurol. 2001 Dec; 172(2):482-92.

48. Okuyama N, Nakao Y, Takayama S, Toyama Y. Effect of number of fascicle on axonal regeneration in cable grafts. Microsurgery. 2004; 24(5):400-7.
49. Prodanov D, Feirabend HK. Morphometric analysis of the fiber populations of the rat sciatic nerve, its spinal roots, and its major branches. J Comp Neurol. 2007 Jul 1;503(1):85-100.
50. Wang W, Itoh S, Matsuda A, Aizawa T, Demura M, Ichinose S, Shinomiya K, Tanaka. J.Enhanced nerve regeneration through a bilayered chitosan tube: the effect of introduction of glycine spacer into the CYIGSR sequence. J Biomed Mater Res A. 2008 Jun 15;85(4):919-28.

Japanese Journal of Applied Physics **52** (2013) 07HF24 **REGULAR PAPER**
http://dx.doi.org/**10.7567/JJAP.52.07HF24**

Calibration Method in Elasticity Evaluation of Regenerating Cartilage Based on Ultrasonic Particle Velocity

Naotaka Nitta[1]*, Koji Hyodo[1], Masaki Misawa[1], Kazuhiko Hayashi[1], Yoshio Shirasaki[1], Kazuhiro Homma[1], and Tsuyoshi Shiina[2]

[1]*Human Technology Research Institute, National Institute of Advanced Industrial Science and Technology (AIST), Tsukuba, Ibaraki 305-8564, Japan*
[2]*Human Health Science, Graduate School of Medicine, Kyoto University, Kyoto 606-8507, Japan*
E-mail: n.nitta@aist.go.jp

Received November 23, 2012; accepted April 30, 2013; published online July 22, 2013

It is important in regenerative medicine to evaluate the maturity of regenerating tissue. In the maturity evaluation of regenerating cartilage, it is useful to measure the temporal change in elasticity because the maturity of regenerating tissue is closely related to its elasticity. In this study, a quantitative elasticity evaluation of extracted regenerating cartilage samples, which is based on the laser Doppler measurement of ultrasonic particle velocity and calibration, was experimentally investigated using agar-based phantoms with different Young's moduli and regenerating cartilage samples extracted from beagles in animal experiments. The experimental results verified the feasibility of the proposed method for the elasticity evaluation of regenerating cartilage samples. © 2013 The Japan Society of Applied Physics

1. Introduction

The quantitative evaluation of cartilage has become important with the aging of the population. For example, osteoarthritis (OA) is one of the most common disorders found in elderly people. In degenerative cartilage, the tension of the superficial layer of the collagen fiber decreases gradually.[1–4] The status of cartilage is evaluated with various methodologies. For in vitro evaluations of cartilage using ultrasound, acoustic microscopy,[5–8] sound speed measurement,[9–12] attenuation measurement,[13] reflected wave or backscatter analysis,[14–19] and an elastographic compressive approach based on echo shift measurement due to cartilage compression,[20,21] have been studied. For in vivo evaluations of cartilage, reflected wave analysis, evaluation of the roughness of the cartilage surface, thickness measurement, and power Doppler evaluation using an ultrasound diagnosis device have been studied.[22–26] Moreover, as a less invasive approach, reflected wave analysis using intravascular ultrasound has also been studied.[27] A more direct approach for mechanical property assessment is a mechanical compression-based method. One of the most important properties of cartilage is its mechanical property including elasticity or viscoelasticity. Therefore, some methods[28–30] might also be promising for evaluating the mechanical properties of cartilage. However, since no speckle pattern typically appears in an ultrasound image of cartilage, it would be difficult for elasticity imaging methods based on speckle tracking to evaluate the elasticity of cartilage.

On the other hand, as a solution to recover degenerated or deficient cartilage, regenerative medicine has been addressed. In typical regenerative medicine for cartilage recovery, a cell-seeded scaffold is cultured over a period of time and then the cultured scaffold is transplanted into the body. Here, evaluations of the cultured scaffold before and after transplantation are essential for ensuring its adequate maturity before and after transportation. In the maturity evaluation of regenerating cartilage, it is useful to measure the temporal change in elasticity because the maturity of regenerating tissue is closely related to its elasticity. For the maturity evaluation, sound speed and attenuation measurements using acoustic microscopy has been reported.[31] On the other hand, since the cultured scaffold before transplantation is the sole material, nondestructive and noncontact measurements are required for elasticity evaluation.

Therefore, with the evaluation of a cultured scaffold sample before transplantation in mind, we previously proposed an elasticity evaluation method for extracted regenerating cartilage samples, which is based on ultrasound particle velocity measurement using a laser Doppler vibrometer (LDV).[32] In our previous study, a relative elasticity evaluation was performed using the inverse of strain (IS) as an index. However, for quantitative evaluations, calibration is required. In this study, a quantitative elasticity evaluation method for extracted regenerating cartilage samples, which is based on the laser Doppler measurement of ultrasonic particle velocity and calibration, was experimentally investigated using agar-based phantoms with different elastic moduli and regenerating cartilage samples extracted from beagles in animal experiments.

2. Calibration Method

In this study, with the aim of simplifying the problem of elasticity evaluation for cartilage tissue, the cartilage tissue is assumed to be a nearly incompressible, isotropic and linear elastic body. In other words, it is assumed that the effect of shear modulus is sufficiently small and negligible, although it is not zero.

Figure 1 shows the principle of the proposed method. Here, a series of ultrasound pulses are irradiated from the bottom of the sample and the particle velocity on the sample surface is measured. Here, only the longitudinal wave propagation is considered, and it is assumed that the whole cartilage tissue sample is homogeneous. Since the particle velocity is continuous at the boundary between media with different acoustic impedances, the particle velocity measured at the surface boundary of the sample is equivalent to that inside the sample. From the above assumptions, when only the plane progressive wave of longitudinal waves propagates in the homogeneous cartilage sample, the particle velocity v_i is expressed as

